CHEMMEDCHEM

DOI: 10.1002/cmdc.201100568

Chromenopyrazoles: Non-psychoactive and Selective CB_1 Cannabinoid Agonists with Peripheral Antinociceptive Properties

Jose Cumella,[a] Laura Hernández-Folgado,[a] Rocio Girón,[b] Eva Sánchez,[b] Paula Morales,[a] Dow P. Hurst,[c] Maria Gómez-Cañas,[d] Maria Gómez-Ruiz,[d] Diana C. G. A. Pinto,[e] Pilar Goya,[a] Patricia H. Reggio,[c] María Isabel Martin,[b] Javier Fernández-Ruiz,[d] Artur M. S. Silva,[e] and Nadine Jagerovic*[a]

The unwanted psychoactive effects of cannabinoid receptor agonists have limited their development as medicines. These CB_1-mediated side effects are due to the fact that CB_1 receptors are largely expressed in the central nervous system (CNS). As it is known that CB_1 receptors are also located peripherally, there is growing interest in targeting cannabinoid receptors located outside the brain. A library of chromenopyrazoles designed analogously to the classical cannabinoid cannabinol were synthesized, characterized, and tested for cannabinoid activity. Radioligand binding assays were used to determine their affinities at CB_1 and CB_2 receptors. Structural features required for CB_1/CB_2 affinity and selectivity were explored by molecular modeling. Some compounds in the chromenopyrazole series were observed to be selective CB_1 ligands. These modeling studies suggest that full CB_1 selectivity over CB_2 can be explained by the presence of a pyrazole ring in the structure. The functional activities of selected chromenopyrazoles were evaluated in isolated tissues. In vivo behavioral tests were then carried out on the most effective CB_1 cannabinoid agonist, **13a**. Chromenopyrazole **13a** did not induce modifications in any of the tested parameters on the mouse cannabinoid tetrad, thus discounting CNS-mediated effects. This lack of agonistic activity in the CNS suggests that this compound does not readily cross the blood–brain barrier. Moreover, **13a** can induce antinociception in a rat peripheral model of orofacial pain. Taking into account the negative results obtained with the hot-plate test, the antinociception induced by **13a** in the orofacial test could be mediated through peripheral mechanisms.

Introduction

The three major components of marijuana are Δ^9-tetrahydrocannabinol (Δ^9-THC), cannabidiol (CBD), and cannabinol (CBN).[1] Unlike Δ^9-THC,[2] CBD and CBN are non-psychotropic phytocannabinoids.[3] Δ^9-THC interacts with two well-characterized G-protein-coupled receptors: CB_1 and CB_2.[4,5] The CB_1 receptors are localized with high density in the brain and are also found in peripheral tissues. In contrast, the CB_2 receptors are expressed mainly in immune cells, although they can also be found in the CNS, particularly under pathological circumstances. The activity of the cannabinoid receptors is elicited not only by phytocannabinoids, but also by synthetic ligands and endocannabinoids.[6–9] The only cannabinoid receptor ligands prescribed so far are CB_1/CB_2 receptor agonists. Cesamet (nabilone) and Marinol (Δ^9-THC) are used for the treatment of nausea and vomiting associated with cancer chemotherapy or as anti-emetic agents. Sativex (Δ^9-THC and CBD) is prescribed to relieve spasticity and pain in patients of multiple sclerosis. However, preclinical data indicate that CB_1 and/or CB_2 receptor agonists are useful for diverse therapeutic applications, including pain relief, treatment of intestinal disorders, glaucoma, cancer proliferation, and neurodegenerative diseases.[10–12]

Δ^9-THC and CBN are classical cannabinoids characterized by tricyclic terpenoids bearing a benzopyran moiety (Figure 1).[13] Structure–activity relationship (SAR) studies of Δ^9-THC and Δ^8-THC analogues for CB_1/CB_2 receptors have been widely report-

[a] Dr. J. Cumella, Dr. L. Hernández-Folgado, P. Morales, Prof. Dr. P. Goya, Dr. N. Jagerovic
Instituto de Química Médica, CSIC
Juan de la Cierva 3, 28006 Madrid (Spain)
E-mail: nadine@iqm.csic.es

[b] Dr. R. Girón, Dr. E. Sánchez, Prof. Dr. M. I. Martin
Departamento de Farmacología y Nutrición
Facultad de Ciencias de la Salud, Universidad Rey Juan Carlos
Avda. Atenas S/N, 28922 Alcorcón, Madrid (Spain)

[c] Dr. D. P. Hurst, Prof. Dr. P. H. Reggio
Department of Chemistry and Biochemistry
University of North Carolina Greensboro
Greensboro, NC 27402 (USA)

[d] M. Gómez-Cañas, Dr. M. Gómez-Ruiz, Prof. Dr. J. Fernández-Ruiz
Departamento de Bioquímica y Biología Molecular, Facultad de Medicina
Centro de Investigación Biomédica en Red sobre Enfermedades Neurodegenerativas (CIBERNED)
Instituto Ramón y Cajal de Investigación Sanitaria (IRYCIS)
Universidad Complutense de Madrid, 28040 Madrid (Spain)

[e] Dr. D. C. G. A. Pinto, Prof. Dr. A. M. S. Silva
Department of Chemistry & QOPNA
University of Aveiro, 38210-193 Aveiro (Portugal)

Supporting information for this article is available on the WWW under http://dx.doi.org/10.1002/cmdc.201100568.

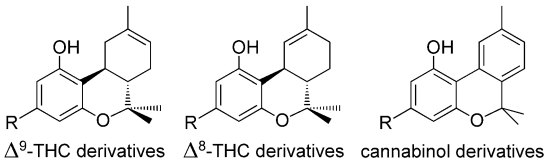

Figure 1. Structures of Δ^9-THC, Δ^8-THC and cannabinol derivatives.

ed.[14–19] It is well established that the C1, C3, and C9 positions play a key role in the binding affinity and pharmacological potency of THCs. Although some of these classical cannabinoids have been reported to show significant selectivity for one of the two receptor types, structural variations within Δ^9-THC have generally resulted in derivatives with high affinity for both CB_1 and CB_2 receptors. Considerable effort has been directed toward the SARs of THCs; however, fewer structural modifications have been made on the structure of cannabinol. Rhee et al.[20] reported the binding and inhibition of adenylyl cyclase by a series of CBN derivatives. Unlike CBN, which was found to be less potent than Δ^9-THC, the 3-dimethylheptyl CBN analogue and 9-hydroxymethyl CBN analogues showed higher affinity and agonist potency than Δ^9-THC at both CB_1 and CB_2 receptors. The presence of alkyl or aryl esters at position 9 of CBN resulted in weak CB_1 and CB_2 binding.[21] Cannabilactones were reported more recently by Khanolkar et al.[22] One of them exhibited high CB_2 receptor affinity, with 500-fold selectivity over the CB_1 receptor. All these considerations taken together, it is clear that the structural requirements for cannabinoid receptor binding by the CBN series differs from those of the THCs.

The pharmacological properties of CBN have also received less attention than the THCs. Analgesic properties of CBN have been reported in various models of pain.[23–26] CBN generally requires higher doses than Δ^9-THC to produce antinociception, but it shows minimal psychomimetic effects.[27,28] One of the main challenges in the design of new cannabinoid ligands is the avoidance of CNS side effects. In 1985 Press and Birnberg[29] reported benzopyrano[4,3-*c*]pyrazoles that did not show neuroleptic activity in locomotor and catalepsy tests. We propose exploration of this scaffold for cannabinoid ligands. In this context, we report herein the contribution of a pyrazole ring in place of the cannabinol phenyl group toward cannabinoid activity.

Results

Chemistry

7-Alkyl-1,4-dihydro-4,4-dimethylchromenopyrazol-9-oles **7**–**15** were prepared from the corresponding resorcinol as shown in Scheme 1. 5-(1′,1′-Dimethyl-*n*-heptyl)-1,3-dihydroxybenzene (**2**) was previously synthesized by demethylation[30] of 5-(1′,1′-dimethyl-*n*-heptyl)-1,3-dimethoxybenzene. The appropriate starting resorcinol was allowed to react with 3,3-dimethylacrylic acid in methanesulfonic acid in the presence of phosphorus pentoxide to form the 7-alkyl-5-hydroxy-2,2-dimethylchroman-4-ones **3** and **4** under microwave heating conditions and using the reagents described by Lim et al.[31] For the α-formylation of **3** and **4**, an alternative procedure to the overnight heating proposed by Press and colleagues[32] yielded the corresponding

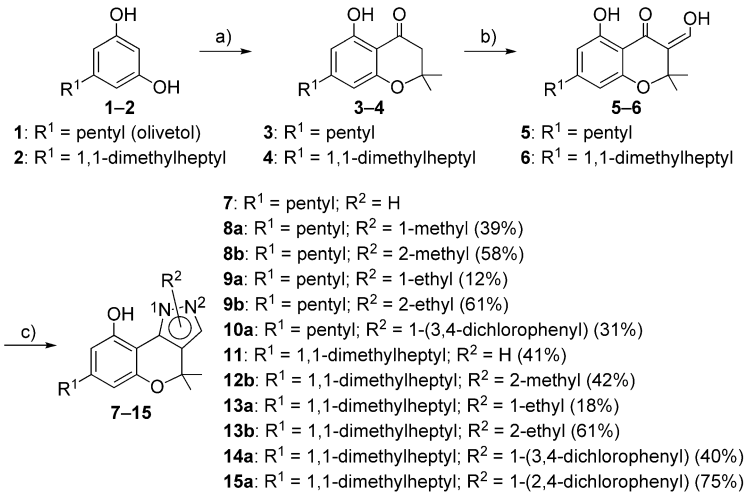

Scheme 1. *Reagents and conditions:* a) 3,3-dimethylacrylic acid, CH_3SO_3H, P_2O_5, 70 °C, MW, 10 min; b) NaH, THF, MW, 46 °C, 20 min, then ethyl formate, THF, MW, 46 °C, 20 min; c) H_2N-NHR_2, EtOH, 16 h, RT or 10 min, MW.

(*Z*)-7-alkyl-5-hydroxy-3-(hydroxymethylen)-2,2-dimetylchroman-4-ones **5** and **6** in 20 min by using microwave irradiation. Condensation of the β-keto aldehydes **5** and **6** with the appropriate hydrazine then gave the corresponding 7-alkyl-1(2),4-dihydro-4,4-dimethylchromeno[4,3-*c*]pyrazol-9-oles **7**–**15**. From methyl- and ethylhydrazines, the two N^1- and N^2-substituted pyrazole isomers (**8a**,**b**; **9a**,**b**; **13a**,**b**) were isolated with an approximate relative ratio from 8:2 to 6:4 (N^1/N^2). However, reaction of β-keto aldehyde **5** or **6** with arylhydrazine resulted in only one isomer being isolated, corresponding to the N^1-arylchromenopyrazole (**10a**, **14a**, and **15a**). The fact that alkylhydrazines give a mixture of N^1- and N^2-substituted 7-alkyl-1(2),4-dihydro-4,4-dimethylchromeno[4,3-*c*]pyrazol-9-oles can be explained by the reaction of *N*′-hydrazine as well as *N*-hydrazine with the aldehyde group of **5** and **6**, giving compounds **8a**,**b**, **9a**,**b**, and **13a**,**b** upon cyclization. For *N*′-arylhydrazines, *N*′-hydrazine is much less nucleophilic than *N*-hydrazine, and this leads to a single isomer, as in the case of **10a**, **14a**, and **15a**.

Biological assays

Competitive binding studies

The compounds reported herein were evaluated in vitro for their ability to displace [^{3}H]CP55940 from human cannabinoid CB_1 and CB_2 receptors transfected into HEK293 EBNA cells. They were first subjected to a preliminary screen at a concen-

Table 1. Binding affinity of chromenopyrazole derivatives **7–15** for hCB$_1$ and hCB$_2$ cannabinoid receptors.

Compd	R^1	R^2	hCB$_1$ K_i [nM][a]	hCB$_2$ K_i [nM][a]	CB$_1$/CB$_2$[c]
7	pentyl	H	4100 ± 800	2010 ± 500	0.5
8a	pentyl	1-methyl	4700 ± 1200	3460 ± 1000	0.7
8b	pentyl	2-methyl	22100 ± 1410	> 40000	–
9a	pentyl	1-ethyl	9610	> 40000	–
9b	pentyl	2-ethyl	> 40000	4450 ± 1015	–
10a	pentyl	1-(3,4-dichlorophenyl)	607 ± 151	> 40000	–
11	1,1-dimethylheptyl	H	28.5 ± 33.6	> 40000	> 1000
12b	1,1-dimethylheptyl	2-methyl	14.2 ± 4.2	> 40000	> 1000
13a	1,1-dimethylheptyl	1-ethyl	4.5 ± 0.8	> 40000	> 1000
13b	1,1-dimethylheptyl	2-ethyl	18.6 ± 4.1	> 40000	> 1000
14a	1,1-dimethylheptyl	1-(3,4-dichlorophenyl)	514 ± 355	270	0.5
15a	1,1-dimethylheptyl	1-(2,4-dichlorophenyl)	5.2 ± 6.0	> 40000	> 1000
SR141716	–	–	7.3 ± 0.9	ND[b]	–
WIN 55,212-2	–	–	45.6 ± 8.6	3.7 ± 0.2	–

[a] Values obtained from competition curves using [^{3}H]CP55940 as radioligand for hCB$_1$ and hCB$_2$ cannabinoid receptors and are expressed as the mean ± SEM of at least three experiments. [b] Not determined. [c] Selectivity ratio for CB$_1$ versus CB$_2$.

tration of 40 μM. A complete dose–response curve was generated for compounds that displaced the radioligand by > 50% in the preliminary screen. Table 1 lists the experimental binding affinities (K_i values) from the respective displacement curves for hCB$_1$ and hCB$_2$ receptors.

The first series to be examined were the 2,4-dihydrochromen[4,3-*c*]pyrazol-9-oles and 1,4-dihydrochromen-[4,3-*c*]pyrazol-9-oles bearing an *n*-pentyl side chain (compounds **7**–**10a**). Excluding **10a**, which binds weakly to the CB$_1$ cannabinoid receptor, the binding data for **7**, **8a**, **8b**, **9a**, and **9b** (Table 1) clearly show that these compounds bind neither the CB$_1$ nor CB$_2$ receptor. As reported,[33] the introduction of a C1′-alkyl substituent to Δ^9-THC, Δ^8-THC, and CBN derivatives leads to an enhancement in affinity for both the CB$_1$ and CB$_2$ receptors. Interestingly, the 1,1-dimethylheptylchromenopyrazole derivatives **11**, **12b**, **13a**, **13b**, and **15a** showed significant to high affinity for CB$_1$ (K_i: 4.5–28.5 nM) whereas they did not bind CB$_2$ at all (K_i: > 40000 nM). This is the first observation of such CB$_1$ receptor selectivity among the cannabinoid ligands with a classical cannabinoid structure. Thus, chromenopyrazoles **11**, **12b**, **13a**, **13b**, and **15a** show an optimal CB$_1$ selectivity relative to the CB$_1$/CB$_2$ binding data reported for Δ^9-THC, Δ^8-THC, and CBN derivatives.

With respect to substitution on the pyrazole ring, the K_i values remained generally similar among the 1,1-dimethylheptyl analogues, except for the N^1-3,4-dichlorophenyl moiety: compound **14a** exhibited decreased affinity for both CB$_1$ and CB$_2$ receptors, with a loss of CB$_1$ selectivity.

Isolated tissue assays

The functional activity of **11**, **13a**, and **13b** was tested on mouse vas deferens, a tissue where CB$_1$ cannabinoid receptors are expressed, and thus which is commonly used to study and characterize cannabinoid effects, as previously described.[34] Compounds **11**, **13a**, and **13b** inhibited the electrically evoked contractile response of this tissue. In agreement with its high affinity for the CB$_1$ receptor, **13a** exhibited the highest effectiveness (Figure 2). These three ligands were less effective than

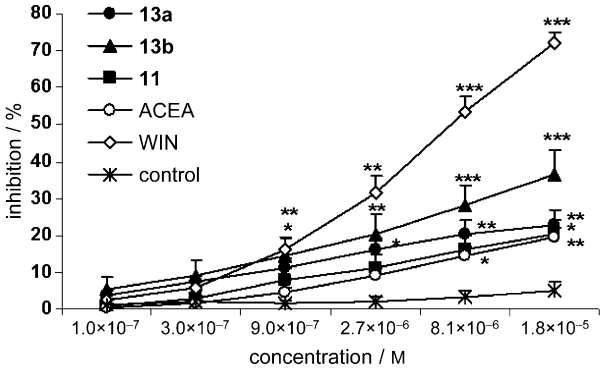

Figure 2. Effect of WIN 55,212-2 (WIN), arachidonyl-2-chloroethylamide (ACEA) and compounds **11**, **13a**, and **13b** in mouse vas deferens. Values represent the mean ± SEM (n = 6–8) of modification of the electrically induced contraction of vas deferens tissue by the addition of increasing concentrations of vehicle (control), WIN, ACEA, or test compounds. Significant differences versus control are indicated: *p < 0.05, **p < 0.01, ***p < 0.001 (two-way ANOVA followed by Bonferroni's post-hoc test).

WIN 55,212-2 (WIN); however, their effect was similar to that of arachidonyl-2-chloroethylamide (ACEA), a CB$_1$-selective agonist commonly used to characterize cannabinoid effects. Considering that compound **13a** showed the most interesting profile as potential CB$_1$ agonist, the inhibition of its effect was tested by adding the cannabinoid antagonist AM251 to the organ bath 10 min before the addition of the tested compound. As illustrated in Figure 3, the effect of **13a** was clearly decreased by this CB$_1$-selective antagonist. Moreover, the CB$_2$-selective antagonist AM630 was similarly tested, and it did not block the effect of compound **13a** (data not shown).

In vivo bioassays

Cannabinoid tetrad

Psychoactive cannabinoids dose-dependently modify spontaneous activity, antinociceptive response, rectal temperature, and catalepsy in mice.[35] Effects of WIN and **13a** on the canna-

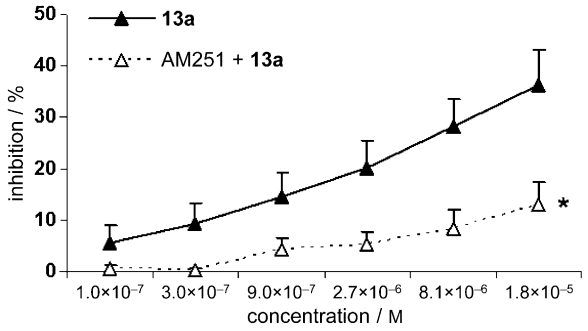

Figure 3. Effect of AM251 in blocking the activity of compounds **13a**. Values represent the mean ± SEM ($n = 6$) inhibition of electrically induced contraction of mouse vas deferens induced by the addition of increasing concentrations of compound **13a** in control tissues or in tissues incubated with AM251. Significant difference versus control tissues: $*p < 0.05$ (two-way ANOVA followed by Bonferroni's post-hoc test).

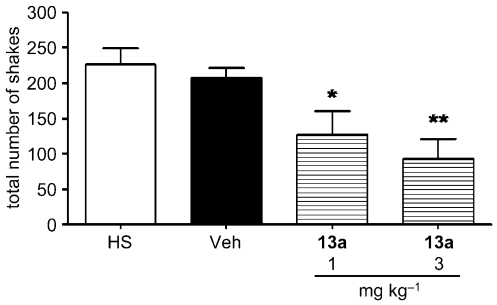

Figure 5. Antinociceptive effect of compound **13a** (1 and 3 mg kg^{-1}), i.p. administered, 30 min before HS injection. Bars show the total number of shakes (mean ± SEM); $*p < 0.05$, $**p < 0.01$ versus vehicle (Veh); one-way ANOVA, $n \geq 6$.

binoid tetrad were evaluated. Intraperitoneal (i.p.) administration of WIN (at 2.5 and 5 mg kg^{-1}) induced antinociceptive effect in the hot-plate test, hypothermia, catalepsy, and a decrease in locomotor activity, whereas compound **13a** (at 5 and 10 mg kg^{-1}) did not modify any of these signs of cannabinoid tetrad activity (Figure 4). This result suggests that **13a** lacks any significant CNS effects.

Orofacial pain model

Hypertonic saline (HS) injection in the masseter of rats produced a paw-shaking behavior. This nociceptive behavior was decreased by i.p. administration of compound **13a** (at 1 and 3 mg kg^{-1}), suggesting that **13a** is active in this pain model (Figure 5), acting at CB_1 receptors located outside the CNS.

Molecular modeling

The CB_1 cannabinoid receptor selectivity observed for the 1,1-dimethylheptylchromenopyrazoles offers the opportunity to explore structural features required for CB_1/CB_2 selectivity by molecular modeling. Conformational analysis of *N*-H-chromenopyrazole **11** and the two *N*-methylchromenopyrazole regioisomers **13a** and **13b** was first performed to determine the global minimum-energy conformation of each, as well as other minimum-energy conformations. With respect to *N*-H-chromenopyrazole **11**, two tautomers (**11a** and **11b**, Figure 6) were considered. Although conformational analysis of **11a** shows that it is more stable than **11b** by 1.9 kcal mol^{-1}, both tautomers were taken into consideration for docking studies.

Figure 7 illustrates the global minimum-energy conformers of tautomers **11a** and **11b**, and regioisomers **13a** and **13b**. The global energy minima of these four compounds were then docked by using a model of the active state (R*) of the cannabinoid receptors CB_1 and CB_2.[36,37] These models include the extracellular and intracellular loops, the N terminus (truncated in CB_1) and the C terminus, including the intracellular helix portion of each receptor, termed helix 8. CB_1 and CB_2 receptor docking studies were performed in the same binding site described for HU210[38] and for AM841[39,40] respectively.

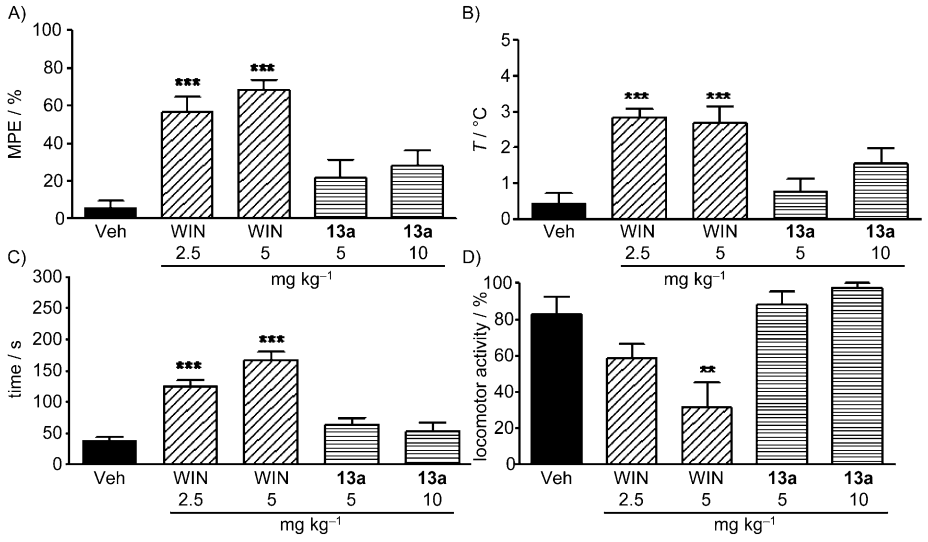

Figure 4. Effect of WIN 55,212-2 (WIN) (2.5 and 5 mg kg^{-1}) and compound **13a** (5 and 10 mg kg^{-1}) in the mouse cannabinoid tetrad. Mice were tested for analgesia by A) hot-plate assay, B) rectal temperature, C) catalepsy on a ring, and D) locomotor activity via rotarod test. $**p < 0.01$, $***p < 0.001$ versus vehicle (Veh); one-way ANOVA, $n \geq 10$.

Chromenopyrazole–cannabinoid receptor docking studies

Tautomer 11b–CB_1R*

The energy-minimized **11b**–CB_1R* complex is illustrated in Figure 8. Lys3.28(192) was used as the primary interaction site for CB_1 docking studies reported herein.[41] The phenolic oxygen atom of **11b** is engaged in a hy-

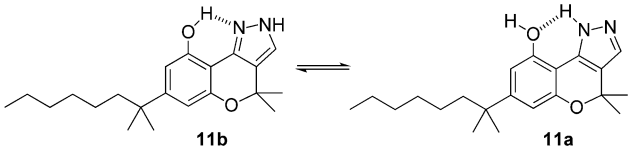

Figure 6. Structures of the two tautomers **11 b** and **11 a**.

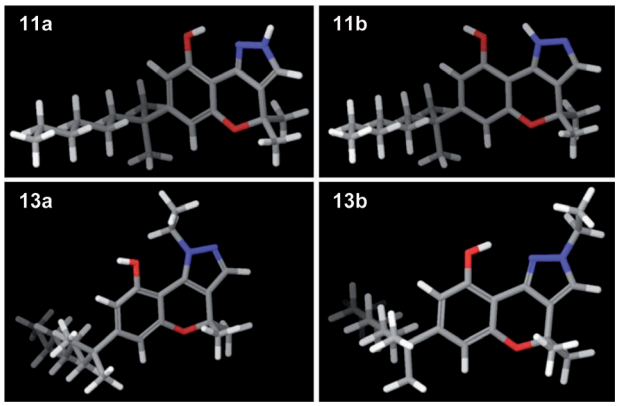

Figure 7. Minimum-energy conformers of tautomers **11 a**, **11 b**, **13 a**, and **13 b**.

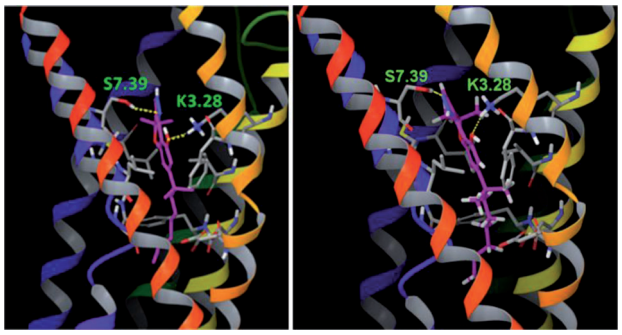

Figure 8. Binding site of **11 b** (left, in pink) and **11 a** (right, in pink) in the CB_1R^* model. The amino acid residues interacting with the ligand are shown in grey. Yellow dashed lines indicate hydrogen bonding interactions.

drogen bond with Lys3.28(192) as reported for the HU210–CB_1R^* binding model [H-bond (N–O) $d = 2.78$ Å, ∢ (N–H–O) = 150°]. The N^2-pyrazole nitrogen atom is involved in a hydrogen bond with Ser7.39(383) [H-bond (N–O) $d = 3.15$ Å, ∢ (O–H–N) = 142°]. Ligand **11 b** exhibits the greatest pairwise interaction energy with Lys3.28(192) (−11.88 kcal mol^{-1}), followed by Leu7.43(387) (−5.64 kcal mol^{-1}), Cys7.42(386) (−5.61 kcal mol^{-1}), and Asn7.45(389) (−5.43 kcal mol^{-1}). Coulombic energy dominates the overall pairwise energy of interaction in the case of Lys3.28(192), whereas van der Waals energy is predominant for Leu7.43(387), Cys7.42(386), and Asn7.45(389). The interaction with Ser7.39(383) was found to be only −4.48 kcal mol^{-1}, indicating a weak hydrogen bond with the N^2-pyrazole nitrogen. The tautomer **11 b** also has significant interactions with Asp2.50(163) (−4.99 kcal mol^{-1}) with van der Waals and coulombic contributions, and with Val3.32(196) (−4.97 kcal mol^{-1}), dominated by van der Waals interactions. The energy difference between the initially docked **11 b** conformation and the final conformation in the energy-minimized complex was found to be 6.69 kcal mol^{-1} at the Hartree–Fock (HF) 6-31G* level. The overall interaction energy for **11 b** at CB_1 was found to be −56.52 kcal mol^{-1} (see table S1 in the Supporting Information).

Tautomer 11 a–CB_1R^*

The docking of tautomer **11 a** in the CB_1R^* receptor model revealed a similar occupation of the binding site, with similar hydrogen bonds involving Lys3.28(192) and Ser7.39(383) as shown in Figure 8. As for the **11 b**–CB_1R^* complex, **11 a** has the greatest pairwise interaction energy with Lys3.28(192) (−11.02 kcal mol^{-1}), and significant interactions with Cys7.42(386) (−6.22 kcal mol^{-1}), Asp2.50(163) (−6.03 kcal mol^{-1}), Leu7.43(387) (−5.20 kcal mol^{-1}), Asn7.45(389) (−5.13 kcal mol^{-1}), and Val3.32(196) (−4.40 kcal mol^{-1}). However, the interaction energy with Ser7.39(383) (−10.88 kcal mol^{-1}) in the **11 a**–CB_1R^* complex was found to be much stronger than for **11 b**. The energy difference between the initially docked **11 a** conformation and the final conformation in the energy-minimized complex was observed to be 6.51 kcal mol^{-1} at the HF 6-31G* level. The overall interaction energy for **11 a** at CB_1 was found to be −63.92 kcal mol^{-1} (see table S1 in the Supporting Information). Taken together, the energies of interaction of **11 a** and **11 b** at CB_1 suggest that **11 a** is the preferred tautomeric form for **11** binding at CB_1.

Compound 13 b–CB_1R^*

In the energy-minimized **13 b**–CB_1R^* complex as illustrated in Figure 9, **13 b** forms two hydrogen bonds with Lys3.28(192). The first involves Lys3.28(192) as hydrogen donor to the phenolic oxygen atom of **13 b** [H-bond (N–O) $d = 2.75$ Å, ∢ (N–H–O) = 152°]). The second interaction involves Lys3.28(192) hydrogen bonding with the pyrazole N^2 atom [H-bond (N–N) $d = 3.10$ Å, ∢ (N–H–N) = 132°]. This pyrazole N^2 atom also forms a hydrogen bond with Ser7.39(383) [H-bond (N–O) $d = 3.15$ Å, ∢ (O–H–N) = 134°]. However, this interaction is weaker than in the CB_1R^* complex with **11** and **13 a**. The ligand **13 b** has its

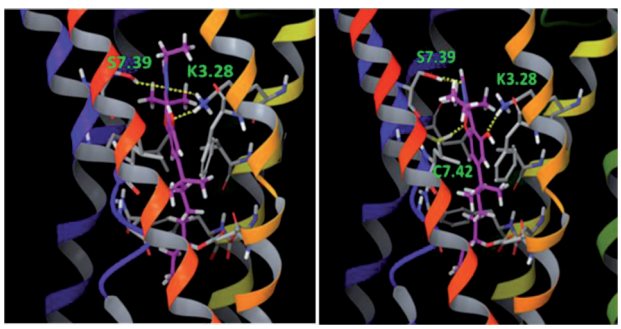

Figure 9. Binding site of **13 a** (left, in pink) and **13 b** (right, in pink) in the CB_1R^* model. The amino acid residues interacting with the ligand are shown in grey. Yellow dashed lines indicate hydrogen bonding interactions.

greatest pairwise interaction energy with Lys3.28(192) (−14.34 kcal mol^{-1}, mainly coulombic energy), followed by Asn7.45(389) (−5.19 kcal mol^{-1}), Leu7.43(387) (−5.13 kcal mol^{-1}), and Cys7.42(386) (−4.76 kcal mol^{-1}), which are predominantly through van der Waals interactions. The **13b**–CB_1R* complex also has significant interactions with Val3.32(196) (−4.72 kcal mol^{-1}) and Asp2.50(163) (−4.70 kcal mol^{-1}). The energy difference between the initially docked conformation of **13b** and the final conformation in the energy-minimized complex was found to be 5.13 kcal mol^{-1} at the HF 6-31G* level. The overall interaction energy for **13b** at CB_1 was found to be −59.92 kcal mol^{-1} (see table S2 in the Supporting Information).

Compound 13a–CB_1R*

The main interactions of the energy-minimized **13a**–CB_1R* complex are shown in Figure 9. As observed for **11a**, **11b**, and **13b**, Lys3.28(192) forms a hydrogen bond with the phenolic oxygen atom of **13a** [H-bond (N–O) d = 2.70 Å, ∢(N–H–O) = 166°]. The N^2 atom of the pyrazole in **13a** hydrogen bonds with Ser7.39(383), as a hydrogen bond acceptor [H-bond (N–O) d = 2.80 Å, ∢(O–H–N) = 160°]. Interestingly, an additional hydrogen bond between the pyran ring oxygen and Cys7.42(386) was revealed in the **13a**–CB_1R* complex [H-bond (S–O) d = 2.91 Å, ∢(S–H–O) = 172°]. The significant increase in pairwise interaction energy with Cys7.42(386) (−7.01 kcal mol^{-1}) relative to the other complexes presented herein (**11a**, **11b**, and **13b**) is a consequence of this additional hydrogen bond. Ligand **13a** exhibits the greatest interaction energy with Lys3.28(192) (−13.83 kcal mol^{-1}), followed by the hydrogen bond interaction with Ser7.39(383) (−7.47 kcal mol^{-1}) and Phe2.57(170) (−5.30 kcal mol^{-1}). The Phe2.57(170) interaction has significant van der Waals and coulombic contributions and seems to have arisen from the interaction of the phenolic ring hydrogen atoms with the aromatic ring of the phenylalanine. The **13a**–CB_1R* complex also has significant interactions with Leu7.43(387) (−7.43 kcal mol^{-1}), Asp2.50(163) (−6.22 kcal mol^{-1}), Asn7.45(389) (−4.97 kcal mol^{-1}), and Val3.32(196) (−4.94 kcal mol^{-1}). The energy difference between the initially docked **13a** conformation and the final conformation in the energy-minimized complex was found to be 7.39 kcal mol^{-1} at the HF 6-31G* level. The overall interaction energy for **13a** at CB_1 was found to be −69.16 kcal mol^{-1} (see table S2 in the Supporting Information). Taken together with the results for **13b** above, these docking studies indicate that the interaction of **13a** at CB_1 is more energetically favorable than those of its positional isomer.

Compounds 11a–, 11b–, 13a–, and 13b–CB_2R*

Compounds **11a**, **11b**, **13b**, and **13a** were also docked in the previously reported advanced CB_2R* model[37,40,42] at the AM841 binding site.[40] The CB_2 receptor model contains a salt bridge between D275 (Asp275) in the EC3 loop and K3.28 [Lys3.28(109)]. Docking studies of the chromenopyrazoles **11a**, **11b**, **13a**, and **13b** revealed a steric clash between the pyrazole moiety of the structures and the ionic lock as illustrated in Figure 10. This result suggests that the presence of the pyrazole plays a key role in the selectivity of compounds **11** and **13** for the CB_1 cannabinoid receptor.

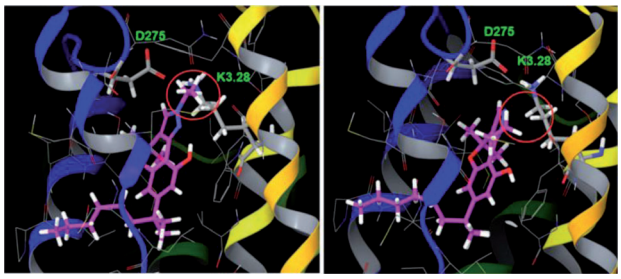

Figure 10. Binding site of **13b** (left, in pink) and **13a** (right, in pink) in the CB_2R* model. The D275–K3.28(109) ionic lock is shown in grey. The red circles indicate steric clash.

Discussion and Conclusions

Although the first generation of classical cannabinoids showed potent activity in vivo, they lacked CB_1/CB_2 selectivity and most of them are psychoactive. These CB_1-mediated side effects are due to the fact that CB_1 receptors are largely expressed in the CNS. Thus, the unwanted psychoactive effects of cannabinoid receptor agonists have limited their development as medicines. Because it is known that CB_1 receptors are also located peripherally,[43] there is a growing interest in targeting cannabinoid receptors located outside the brain. For this reason, it is important to develop new non-psychoactive cannabinoids that do not cross the blood–brain barrier, but act on peripherally located cannabinoid receptors. The chromenopyrazoles presented herein were designed in analogy to CBN, which is a CB_1/CB_2 cannabinoid ligand. The binding data show that the 1,1-dimethylheptyl side chain on this scaffold is necessary for high affinity. The ligand binding studies resulted in K_i values of 4.5–28.5 nM for the 1,1-dimethylheptyl analogues **11**, **12b**, **13a**, **13b**, and **15a** at hCB_1 receptors. Notably, these 1,1-dimethylheptyl analogues do not show affinity for hCB_2 receptors (K_i: >40000 nM). Unlike the major members of the classical cannabinoid family that lack full selectivity for CB_1 or CB_2, the chromenopyrazole structure has a determinant influence on CB_1 selectivity. These results suggest that such selectivity can be explained by the presence of a pyrazole ring in the structure. However, the substituent on the pyrazole may play a major role in the binding to both receptors. Thus, we observed that the 1-(3,4-dichlorophenyl) substituent (compound **14a**) significantly disrupts CB_1 receptor selectivity with a loss of affinity for CB_1 and a moderate affinity for the CB_2 receptor.

As assessed by modeling studies, the 1,1-dimethylheptyl-chromenopyrazoles **11a**, **11b**, **13a**, and **13b** revealed a similar occupation of the HU210/CP55940 binding site in the CB_1 receptor model. The phenolic hydroxy group of **11a**, **11b**, **13a**, and **13b** is crucial for the interaction with CB_1R*, due to a hydrogen bond with Lys3.28(192). This residue has been shown to be critical for the binding of both classical and endocanna-

binoids.[41] Furthermore, interaction with Ser7.39(383) was found to be the main one for the pyrazole moiety, particularly for the **13a**–CB_1R* complex. The Ser7.39(383) residue has been reported to be crucial for the binding of the CB_1 agonist CP55940.[38]

While K3.28 in CB_1 has been reported to be critical for the binding of non-classical, classical, and endocannabinoids,[41] mutation of the equivalent residue in CB_2, K3.28(109) has no effect on the binding of any cannabinoid ligand.[44] An important sequence divergence in the EC3 loop of the CB_2 model (TTLS**D**QVKK) versus the CB_1 model (GKMN**K**LIKT) has been reported.[40] The CB_2R* model suggests a salt bridge formed between Asp275 and Lys3.28(109) that makes K3.28 unavailable for ligand interaction. In our CB_2R* docking, this salt bridge causes a steric clash with the pyrazole moiety of **11a**, **11b**, **13a**, or **13b** due to the rigidity and planarity of the heterocycle. Therefore, these results suggest that the pyrazole moiety in these compounds is responsible for the CB_1 selectivity over CB_2.

Compounds **13a** and **13b** are positional isomers of each other, differing in the placement of an ethyl substituent (N^1, **13a**; N^2, **13b**). Interestingly, the interaction energies of **13a** and **13b** with CB_1 calculated herein follow the same trend as their CB_1 affinities (**13a**: $E_{int} = -69.16$ kcal mol^{-1}, $K_i = 4.5$ nM versus **13b**: $E_{int} = -59.92$ kcal mol^{-1}, $K_i = 18.6$ nM).

The chromenopyrazoles **11**, **13a**, and **13b** were tested in functional in vitro assays. Among them, **13a** acted as the most effective cannabinoid agonist. Its effect was significantly and almost completely inhibited by the CB_1 antagonist AM251 but not by the CB_2 antagonist AM630. Compound **13a** was then selected for carrying out behavioral tests in vivo. It did not induce modifications in any of the tested parameters on the mouse cannabinoid tetrad, thus discounting CNS-mediated effects. This lack of agonistic activity in the CNS suggests that these compounds do not readily cross the blood–brain barrier.

To study other possibilities of antinociception, compound **13a** was tested in another pain model. We chose a model of orofacial pain in rat (nocive stimulation of the masseter by injection of hypertonic saline); in this model it is known that other drugs such as opioids can induce antinociception via peripheral mechanisms.[45,46] In this test, **13a** was able to decrease the nociceptive response. Remarkably, a different result was obtained from the hot-plate test; from these data it could be suggested that the antinociception induced by compound **13a** in the orofacial test may be mediated through peripheral mechanisms.

Experimental Section

Chemistry

Commercially available starting materials and reagents were used as supplied. Reactions conducted under anhydrous conditions were performed under N_2 atmosphere in solvents dried over $CaCl_2$ (THF) or Na/benzophenone (THF). Microwave-mediated syntheses were performed using an 800 W Ethos Synth microwave (Milestone Inc.) and a CEM Biotage microwave. Column chromatography was performed using silica gel 60 (230–400 mesh). Analytical HPLC–MS analysis was performed on a Waters 2695 HPLC system equipped with a Photodiode Array 2996 coupled to a Micromass ZQ 2000 mass spectrometer (ESIMS), using a Waters X-bridge C_{18} column (3.5 μm, 2.1×100 mm) and 30 min gradient A: CH_3CN/0.08% formic acid, B: H_2O/0.05% formic acid, visualizing at $\lambda = 254$ nm. ^{1}H and ^{13}C NMR spectra were recorded on a Bruker 300 (300 and 75 MHz) at 25 °C. Samples were prepared as solutions in deuterated solvent and referenced to internal nondeuterated solvent peak. Chemical shifts (δ) are expressed in ppm downfield of tetramethylsilane. Elemental analyses were determined with a LECO CHNS-932 instrument. Melting points were determined on an MP70 Reichert Jung Thermovar apparatus and are uncorrected. The purity of final compounds was determined by HPLC–MS and elemental analyses performed with the respective aforementioned instrumentation.

5-(1,1-Dimethylheptyl)-1,3-dihydroxybenzene[30] (2): BBr_3 (1 M in CH_2Cl_2, 19 mL, 19 mmol) was added to a solution of 5-(1,1-dimethylheptyl)-1,3-dimethoxybenzene (0.45 g, 1.9 mmol) in dry CH_2Cl_2 at −16 °C under N_2 in the dark. The reaction mixture was allowed to warm to room temperature and was stirred for 20 h. CH_3OH was then added carefully at 0 °C until the mixture reached pH 7. The solvent was removed in vacuo, and the crude was purified by chromatography on silica gel (EtOAc) to give the title compound as a white solid (0.33 g, 73%); mp: 88–91 °C (98 °C);[30] ^{1}H NMR ($CDCl_3$): $\delta = 6.35$–6.45 (m, 2H, 4-H), 6.16 (m, 1H, 2-H), 4.65 (bs, 2H, OH), 1.45–1.50 (m, 2H, 2′-H), 1.22 (s, 6H, CH_3), 1.21–1.10 (m, 6H, 3′-H, 4′-H, 5′-H), 1.03 (bs, 2H, 6′-H), 0.84 ppm (t, $J = 6.5$ Hz, 3H, CH_3); ^{13}C NMR ($CDCl_3$): $\delta = 163.2$ (3-C), 154.0 (5-C), 111.2 (4-C), 101.3 (2-C), 45.0 (2′-C), 35.3, 31.1, and 23.9 (3′-C, 4′-C, 5′-C), 29.8 (8′-C), 25.1 (6′-C), 14.8 ppm (7′-C); HPLC–MS: [A, 20→80%], $t_R = 14.0$ min, (90%); MS (ES$^+$, *m/z*) 237 (100%) $[M+H]^+$; Anal. calcd for $C_{15}H_{24}O_2$: C 76.23, H 10.24, found: C 76.10, H 10.18.

5-Hydroxy-2,2-dimethyl-7-pentylchroman-4-one[29] (3): Olivetol (0.48 g, 2.7 mmol) and 3,3-dimethylacrylic acid (0.27 g, 2.7 mmol) were added to a mixture of P_2O_5 (0.23 g, 1.6 mmol) and methanesulfonic acid (4.6 mL, 72 mmol) under N_2 at room temperature. The mixture was then irradiated by microwave at 70 °C in a sealed reactor for 10 min. The mixture was poured onto water/ice and then extracted with CH_2Cl_2. The organic layer was dried over $MgSO_4$. After removal of the solvent, the crude was purified by chromatography on silica gel (EtOAc) to give the title compound as an orange oil (0.34 g, 48%); ^{1}H NMR ($CDCl_3$): $\delta = 6.32$ (d, $J = 2.4$ Hz, 1H, 8-H), 6.26 (d, $J = 2.4$ Hz, 1H, 6-H), 2.98 (t, $J = 7.1$ Hz, 2H, 1′-H), 2.66 (s, 2H, 3-H), 1.48–1.53 (m, 2H, 2′-H), 1.44–1.38 (m, 2H, 3′-H), 1.41 (s, 6H, $OC(CH_3)_2$), 1.30–1.40 (m, 2H, 4′-H), 0.87 ppm (t, $J = 6.9$ Hz, 3H, 5′-H); ^{13}C NMR ($CDCl_3$): $\delta = 191.2$ (4-C), 161.9 (5-C), 159.7 (8a-C), 147.6 7-C), 110. 2 (8-C), 109.9 (6-C), 100.1 (4-C), 76.4 (2-C), 48.3 (3-C), 33.3 (1′-C), 30.1 (3′-C), 28.1 (2′-C), 24.8 ($OC(CH_3)_2$), 20.7 (4′-C), 12.2 ppm (5′-C); HPLC–MS: [A, 20→80%], $t_R = 17.6$ min, (90%); MS (ES$^+$, *m/z*) 263 (100%) $[M+H]^+$; Anal. calcd for $C_{16}H_{22}O_3$: C 73.25, H 8.45, found: C 72.98, H 8.71.

7-(1,1-Dimethylheptyl)-5-hydroxy-2,2-dimethylchroman-4-one (4): Prepared from **2** (0.37 g, 1.6 mmol), P_2O_5 (0.18 g, 1.3 mmol), methanesulfonic acid (2.67 mL, 54 mmol), and 3,3-dimethylacrylic acid (1.99 g, 19.9 mmol) by following the procedure described for **3**. Pale-yellow oil (0.34 g, 40%); ^{1}H NMR ($CDCl_3$): $\delta = 6.45$ (d, $J = 1.6$ Hz, 1H, 8-H), 6.37 (d, $J = 1.6$ Hz, 1H, 6-H), 2.71 (s, 2H, 3-H), 1.52–1.59 (m, 2H, 2′-H), 1.46 (s, 6H, $OC(CH_3)_2$), 1.22 (s, 6H, $C(CH_3)_2$), 1.19 (bs, 6H, 3′-H, 4′-H, 5′-H), 1.05 (bs, 2H, 6′-H), 0.87 ppm (m, 3H, 7′-H); ^{13}C NMR ($CDCl_3$): $\delta = 197.9$ (4-C), 163.0 (5-C), 161.7 (8a-C), 156.0 (7-C), 107.0 (8-C), 106.2 (6-C), 105.7 (4-C), 79.1 (2-C), 48.5 (3-C), 41.0 (2′-C), 39.2 (1′-C), 32.1, 27.1 and 23.0 (3′-C, 4′-C and 5′-C), 30.3 ($C(CH_3)_2$), 28.8 ($OC(CH_3)_2$), 25.0 (6′-C), 14.5 ppm (7′-C); HPLC–MS: [A,

80→100%], t_R=4.9 min, (97%); MS (ES^+, *m/z*) 318 (97%) $[M+H]^+$; Anal. calcd for $C_{20}H_{30}O_3$: C 75.43, H 9.50, found: C 75.52, H 9.64.

5-Hydroxy-3-(hydroxymethylen)-2,2-dimethyl-7-pentylchroman-4-one[29] (5): Dry 95% NaH (0.14 g, 6 mmol) was added to a solution of dihydrochroman-4-one **3** (0.17 g, 0.7 mmol) in dry THF under N_2. The reaction mixture was irradiated by microwave at 46 °C in a sealed reactor for 20 min. Ethyl formate (0.96 mL, 12 mmol) was then added, and the mixture was irradiated for an additional 20 min at 46 °C. The solvent was then evaporated under reduced pressure. H_2O was added to the residue. The aqueous solution was extracted with Et_2O and then was neutralized with 1 M HCl and extracted with CH_2Cl_2. The combined organic layers were dried ($MgSO_4$) and evaporated under reduced pressure. Column chromatography on silica gel (hexanes/EtOAc 1:1) afforded the title compound as a pale-yellow oil (0.12 g, 60%); ^{1}H NMR ($CDCl_3$): δ= 13.48 (d, *J*=11.1 Hz, 1H, CHO*H*), 11.36 (s, 1H, 5-OH), 7.34 (d, *J*= 11.1 Hz, 1H, 10-H), 6.32 (d, *J*=1.3 Hz, 1H, 8-H), 6.21 (d, *J*=1.3 Hz, 1H, 6-H), 2.49 (t, *J*=7.6 Hz, 2H, 1′-H), 1.58–1.65 (m, 2H, 2′-H), 1.56 (bs, 6H, 9-H), 1.30–1.19 (m, 4H, 3′-H and 4′-H), 0.88 ppm (t, *J*= 7.2 Hz, 3H, 5′-H); ^{13}C NMR ($CDCl_3$): δ=189.9 (4-C), 162.3 (5-C), 161.9 (CHOH), 159.3 (8a-C), 155.9 (7-C), 114.7 (3-C), 109.8 (8-C), 108.7 (6-C), 105.5 (4-C), 78.7 (2-C), 37.1 (1′-C)), 31.8 (3′-C), 30.4 (2′-C), 28.6 (9-C), 22.9 (4′-C), 14.4 ppm (5′-C); MS (ES^+, *m/z*) 291 (100%) $[M+H]^+$; HPLC–MS: [A, 80→100%], t_R=1.5 min, (99%); MS (ES^+, *m/z*) 318 (97%) $[M+H]^+$; Anal. calcd for $C_{17}H_{22}O_4$: C 70.32, H 7.64, found: C 70.47, H 7.31.

7-(1,1-Dimethylheptyl)-5-hydroxy-3-(hydroxymethylen)-2,2-dimethylchroman-4-one (6): Prepared from **4** (0.17 g, 0.5 mmol), NaH (0.16 g, 6.7 mmol), and ethyl formate (1.44 mL, 2.7 mmol) by following the procedure described for **5**. Column chromatography on silica gel (hexanes/EtOAc 2:1). Pale-yellow oil (0.16 g, 76%); ^{1}H NMR ($CDCl_3$): δ=13.48 (d, *J*=11.6 Hz, 1H, CHO*H*), 11.28 (s, 1H, 5-OH), 7.34 (d, *J*=11.6 Hz, 1H, C*H*OH), 6.46 (d, *J*=1.6 Hz, 1H, 8-H), 6.35 (d, *J*=1.6 Hz, 1H, 6-H), 1.58 (bs, 6H, $OC(CH_3)_2$), 1.22 (bs, 6H, $C(CH_3)_2$), 1.12–1.28 (m, 6H, 3′-H, 4′-H and 5′-H), 1.03 (m, 2H, 6′-H), 0.83 ppm (t, *J*=6.7 Hz, 3H, 7′-H); ^{13}C NMR ($CDCl_3$): δ=189.8 (4-C), 163.1 (5-C), 162.0 (CHOH), 161.9 (8a-C), 159.1 (7-C), 114.8 (3-C), 107.8 (6-C), 106.6 (8-C), 105.2 (4-C), 78.7 (2-C), 44.4 (2′-C), 39.2 (1′-C), 32.1, 30.3 and 25.0 (3′-C, 4′-H and 5′-H), 28.8 ($C(CH_3)_2$), 28.6 ($OC(CH_3)_2$), 23.0 (6′-C), 14.5 ppm (7′-C); HPLC–MS: [A, 20→80%], t_R=22.7 min, (100%); MS (ES^+, *m/z*) 347 (100%) $[M+H]^+$; Anal. calcd for $C_{21}H_{30}O_4$: C 72.80, H 8.73, found: C 73.07, H 8.64.

1,4-Dihydro-4,4-dimethyl-7-pentylchromen[4,3-*c*]pyrazol-9-ol (7): A solution of **5** (40 mg, 0.13 mmol) and anhydrous hydrazine (10 mg, 0.26 mmol) in EtOH (3 mL) was irradiated under microwave for 10 min. The solvent was evaporated, and the crude residue was subjected to chromatography on silica gel (hexanes/EtOAc 2:1) to obtain **7** as a white solid (20 mg, 59%); mp: 133–137 °C; ^{1}H NMR ($CDCl_3$): δ=8.52 (bs, 1H, OH), 7.31 (s, 1H, 3-H), 6.44 (d, *J*=1.5 Hz, 1H, 6-H), 6.37 (d, *J*=1.5 Hz, 1H, 8-H), 2.53 (t, *J*=7.1 Hz, 2H, 1′-H), 1.90–1.76 (m, 8H, $OC(CH_3)_2$ and 2′-H), 1.41–1.31 (m, 4H, 3′-H and 4′-H), 0.86 ppm (t, *J*=6.9 Hz, 3H, 5′-H); ^{13}C NMR ($CDCl_3$): δ=156.1 (9-C), 153.9 (5a-C), 146.3 (7-C), 142.7 (9b-C), 123.4 (3-C), 120.2 (3a-C), 109.4 (6-C), 108.6 (8-C), 101.7 (9a-C), 77.0 (4-C), 36.6 (1′-C), 31.9 (3′-C), 30.9 (2′-C), 29.9 ($OC(CH_3)_2$), 22.9 (4′-C), 14.4 ppm (5′-C); HPLC–MS: [A, 10→100%], t_R=5.9 min, (98%); MS (ES^+, *m/z*) 287 (97%) $[M+H]^+$; Anal. calcd for $C_{17}H_{22}N_2O_2$: C 71.30, H 7.74, found: C 71.01, H 7.47.

1,4-Dihydro-1,4,4-trimethyl-7-pentylchromeno[4,3-*c*]pyrazol-9-ol[29] (8a) and 2,4-dihydro-2,4,4-trimethyl-7-pentylchromeno[4,3-*c*]pyrazol-9-ol[29] (8b): Methylhydrazine (7.00 μL, 0.13 mmol) was added to a solution of **5** (10 mg, 0.03 mmol) in EtOH. The reaction mixture was stirred at room temperature for 16 h. The solvent was evaporated under reduced pressure. The crude oil was purified by column chromatography on silica gel (hexanes/EtOAc 2:1) to isolate the two isomers **8a** and **8b**. Compound **8a** was obtained as an orange oil (4 mg, 39%); ^{1}H NMR ($CDCl_3$): δ=7.32 (s, 1H, 3-H), 6.50 (d, *J*=1.3 Hz, 1H, 6-H), 6.27 (d, *J*=1.3 Hz, 1H, 8-H), 4.11 (s, 3H, N-CH_3), 2.50 (t, *J*=7.7 Hz, 2H, 1′-H), 1.55–1.44 (m, 8H, 2′-H and $OC(CH_3)_2$), 1.31–1.25 (m, 4H, 3′-H and 4′-H), 0.89 (m, 3H, 5′-H); ^{13}C NMR ($CDCl_3$): δ=154.5 (9-C), 149.9 (5a-C), 145.4 (7-C), 132.0 (9b-H), 130.9 (3-C)), 123.1 (3a-C), 111.4(8-C), 109.5 (6-C), 76.4 (4-C), 41.1 (N-CH_3), 38.7 (1′-C), 35.7 (3′-C), 31.4 (2′-C), 27.3 ($OC(CH_3)_2$), 22.5 (4′-C), 14.0 ppm (5′-C); HPLC–MS: [A, 20→80%], t_R=15.1 min, (95%); MS (ES^+, *m/z*) 301 (100%) $[M+H]^+$; Anal. calcd for $C_{19}H_{26}N_2O_2$: C 72.58, H 8.33, found: C 72.81, H 8.26. Compound **8b** was obtained as a pale-yellow oil (6 mg, 58%); ^{1}H NMR ($CDCl_3$): δ=8.31 (s, 1H, OH), 7.09 (s, 1H, 3-H), 6.42 (d, *J*=1.1 Hz, 1H, 6-H), 6.34 (d, *J*= 1.1 Hz, 1H, 8-H), 3.90 (s, 3H, N-CH_3), 2.50 (t, *J*=7.6 Hz, 2H, 1′-H), 1.59 (bs, 6H, $OC(CH_3)_2$), 1.50–1.60 (m, 2H, 2′-H), 1.30–1.18 (m, 4H, 3′-H and 4′-H), 0.95–0.84 (m, 3H, 5′-H); ^{13}C NMR ($CDCl_3$): δ=153.6 (9-C), 153.1 (5a-C), 145.3 (7-C), 142.6 (9b-C), 124.0 (3a-C), 120.3 (8-C), 108.7 (6-C), 108.5 (9a-C), 101.5(9a-C), 76.4(4-C), 38.8 (N-CH_3), 36.2 (1′-C), 31.5 and 22.5 (3′-C and 4′-C), 30.7 (2′-C), 29.6 ($OC(CH_3)_2$), 14.0 (5′-C); HPLC–MS: [A, 20→80%], t_R=19.9 min, (96%); MS (ES^+, *m/z*) 301 (100%) $[M+H]^+$; Anal. calcd for $C_{19}H_{26}N_2O_2$: C 72.58, H 8.33, found: C 72.36, H 8.49.

1-Ethyl-1,4-dihydro-4,4-dimethyl-7-pentylchromeno[4,3-*c*]pyrazol-9-ol (9a) and 2-ethyl-2,4-dihydro-4,4-dimethyl-7-pentylchromeno[4,3-*c*]pyrazol-9-ol (9b): A solution of **5** (40 mg, 0.15 mmol) and ethylhydrazine oxalate (20 mg, 0.15 mmol) in EtOH (3 mL) was irradiated under microwave for 10 min. The solvent was evaporated, and the crude residue was subjected to chromatography on silica gel (hexanes/EtOAc 1:1) to isolate the two isomers **9a** and **9b**. Compound **9a** was obtained as a pale-yellow oil (6.0 mg, 12%); ^{1}H NMR ($CDCl_3$): δ=9.35 (bs, 1H, OH), 7.38 (s, 1H, 3-H), 6.46 (s, 1H, 6-H), 6.45 (s, 1H, 8-H), 4.48 (q, *J*=7.1 Hz, 2H, N*C*$H_2$$CH_3$), 2.50 (t, *J*=7.6 Hz, 2H, 1′-H), 1.66–1.52 (m, 8H, 2′-H and $OC(CH_3)_2$), 1.43 (t, *J*=7.1 Hz, 3H, NCH_2CH_3), 1.28–1.19 (m, 4H, 3′-H and 4′-H), 0.88 (t, *J*=6.7 Hz, 3H, 5′-H); ^{13}C NMR ($CDCl_3$): δ=155.5 (9-C), 151.8 (5a-C), 145.6 (7-C), 132.9 (9b-C), 131.7 (3-C), 122.9 (3a-C), 110.4 (6-C), 109.7 (8-C), 103.1 (9a-C), 76.04(4-C), 48.0 (NCH_2CH_3), 35.7 (1′-C), 31.4 and 22.5 (3′-C and 4′-C), 30.4 (2′-C), 27.2 ($OC(CH_3)_2$), 15.9 (NCH_2CH_3), 14.0 ppm (5′-C); HPLC–MS: [A, 60→100%], t_R=1.6 min, (100%); MS (ES^+, *m/z*) 315 (100%) $[M+H]^+$; Anal. calcd for $C_{23}H_{34}N_2O_2$: C 74.55, H 9.25, found: C 74.63, H 9.19. Compound **9b** was obtained as a yellow solid (0.04 g, 61%); mp: 145–149 °C; ^{1}H NMR ($CDCl_3$): δ=8.38 (s, 1H, OH), 7.12 (s, 1H, 3-H), 6.42 (d, *J*=1.3 Hz, 1H, 6-H), 6.30 (d, *J*=1.3 Hz, 1H, 8-H), 4.17 (q, *J*=7.1 Hz, 2H, N*C*$H_2$$CH_3$), 2.50 (t, *J*=7.1 Hz, 2H, 1′-H), 1.58–1.53 (m, 8H, 2′-H and $OC(CH_3)_2$), 1.48 (t, *J*=7.1 Hz, 3H, NCH_2CH_3), 1.30–1.19 (m, 4H, 3′-H and 4′-H), 0.95–0.81 ppm (m, 3, 5′-H); ^{13}C NMR ($CDCl_3$): δ=153.5 (9-C), 153.0 (5a-C), 145.2 (7-C)), 142.4 (9b-C), 122.3 (3-C), 119.8 (3a-C), 108.7 (8-C), 108.4 (6-C), 101.6 (9a-C), 76.7 (4-C), 47.0 (NCH_2CH_3), 36.2 (1′-C), 31.4 and 22.5 (3′-C and 4′-C), 30.7 (2′-C), 29.6 ($OC(CH_3)_2$), 15.4 (NCH_2CH_3), 14.0 ppm (5′-C); HPLC–MS: [A, 60→100%], t_R=2.3 min, (100%); MS (ES^+, *m/z*) 315 (100%) $[M+H]^+$; Anal. calcd for $C_{23}H_{34}N_2O_2$: C 74.55, H 9.25, found: C 74.23, H 9.41.

1-(3,4-Dichlorophenyl)-1,4-dihydro-4,4-dimethyl-7-pentylchromeno[4,3-*c*]pyrazol-9-ol (10b): Prepared from **5** (14 mg, 0.05 mmol) and 3,4-dichlorophenylhydrazine hydrochloride (10 mg, 0.05 mmol) by following the procedure described for **7**. Column chromatography on silica gel (hexanes/EtOAc 2:1) afforded

10b as an orange solid (7 mg, 31%); mp: 120–124 °C; ^{1}H NMR ($CDCl_3$): δ = 7.57 (d, J = 2.4 Hz, 1H, 2-H_{phenyl}), 7.49 (s, 1H, 3-H), 7.44 (d, J = 8.7 Hz, 1H, 5-H_{phenyl}), 7.24 (dd, J = 2.4 Hz, J = 8.7 Hz, 1H, 6-H_{phenyl}), 6.52 (d, J = 1.2 Hz,1H, 6-H), 6.10 (d, J = 1.2 Hz, 1H, 8-H), 2.53–2.45 (m, 2H, 1′-H), 1.60–1.51 (m, 8H, 2′-H and $OC(CH_3)_2$), 1.30–1.22 (m, 4H, 3′-H and 4′-H), 0.93–0.88 ppm (m, 3H, 5′-H); ^{13}C NMR ($CDCl_3$): δ = 154.5 (9-C), 150.0 (5a-C), 146.3 (7-C), 142.0 (1-C_{phenyl}), 137.9 (3-C), 132.9 (3-C_{phenyl}), 132.2 (9b-C), 131.0 (4-C_{phenyl}), 129.9 (5-C_{phenyl}), 126.0 (2-C_{phenyl}), 124.9 (3a-C), 123.5 (6-C_{phenyl}), 111.2 (8-C), 109.7 (6-C), 102.3 (9a-C), 77.2 (4-C), 36.7 (1′-C), 31.5 and 22.5 (3′-C and 4′-C), 30.3 (2′-C), 27.2 ($OC(CH_3)_2$), 14.0 ppm (5′-C); HPLC–MS: [A, 60→100%], t_R = 2.3 min, (100%); MS (ES$^+$, m/z) 431 (100%) [M+H]$^+$.

1,4-Dihydro-4,4-dimethyl-7-(1,1-dimethylheptyl)chromeno[4,3-*c*]pyrazol-9-ol (11): Prepared from **6** (16 mg, 0.05 mmol) and anhydrous hydrazine (0.01 mL, 0.32 mmol) by following the procedure described for **7**. Column chromatography on silica gel (hexanes/EtOAc 2:1) afforded **11** as an orange oil (7 mg, 41%); ^{1}H NMR ($CDCl_3$): δ = 7.32 (bs, 1H, NH), 6.58 (d, J = 1.5 Hz, 1H, 6-H), 6.51 (d, J = 1.5 Hz, 8-H), 6.48 (s, 1H, 3-H), 1.63 (bs, 6H, $OC(CH_3)_2$), 1.58–1.52 (m, 2H, 2′-H), 1.25 (s, 6H, $C(CH_3)_2$), 1.18 (bs, 6H, 3′-H, 4′-H and 5′-H), 1.12–1.05 (m, 2H, 6′-H), 0.83 ppm (t, J = 6.7 Hz, 3H, 7′-H); ^{13}C NMR: δ = ($CDCl_3$) 153.7 (9-C), 153.5 (5a-C), 153.4 (7-C), 144.1 (9b-C), 129.1 (3-C), 123.4 (3a-C), 106.8 (8-C), 106.5 (6-C), 101.7 (9a-C), 77.0 ($OC(CH_3)_2$), 44.9 (2′-C), 38.4 ($C(CH_3)_2$), 32.2, 30.4, and 30.0 (3′-C, 4′-C and 5′-C), 29.3 ($C(CH_3)_2$), 25.0 ($OC(CH_3)_2$), 23.1 (6′-C), 14.5 ppm (7′-C); HPLC–MS: [A, 80→100%], t_R = 3.1 min, (100%); MS (ES$^+$, m/z) 343 (100%) [M+H]$^+$; Anal. calcd for $C_{21}H_{30}N_2O_2$: C 73.65, H 8.83, found: C 74.01, H, 8.59.

7-(1,1-Dimethylheptyl)-2,4-dihydro-2,4,4-trimethylchromeno[4,3-*c*]pyrazol-9-ol (12b): Prepared from **6** (30 mg, 0.09 mmol) and methylhydrazine (0.02 mL, 0.34 mmol) by following the procedure described for **7**. Column chromatography on silica gel (hexanes/EtOAc 2:1) afforded **12b** as a yellow solid (13 mg, 42%); mp: >300 °C; ^{1}H NMR ($CDCl_3$): δ = 8.23 (s, 1H, OH), 7.09 (s, 1H, 3-H), 6.57 (d, J = 1.6 Hz, 1H, 6H), 6.48 (d, J = 1.6 Hz, 1H, 8-H), 3.90 (s, 3H, NCH_3), 1.63 (s, 6H, $OC(CH_3)_2$), 1.65–1.54 (m, 2H, 3′-H), 1.24 (s, 6H, $C(CH_3)_2$), 1.18–1.09 (m, 6H, 3′-H, 4′-H and 5′-H), 1.10–1.04 (m, 2H, 6′-H), 0.83 ppm (t, J = 6.7 Hz, 3H, 7′-H); ^{13}C NMR ($CDCl_3$): δ = 152.2 (9-C), 151.8 (5a-C), 151.6 (7-C), 141.5 (9b-C), 122.9 (3-C), 119.3 (3a-C), 105.5 (6-C), 105.3 (8-C), 100.2 (9a-C), 76.4 ($OC(CH_3)_2$), 43.5 (NCH_3), 38.9 (2′-C), 38.0 (1′-C), 31.8, 30.0 and 29.7 (3′-C, 4′-C and 5′-C), 28.9 (8′-C), 24.6 ($OC(CH_3)_2$), 22.6 (6′-C), 14.1 ppm (7′-C); HPLC–MS: [A, 80→100%], t_R = 5.9 min, (100%); MS (ES$^+$, m/z) 357 (100%) [M+H]$^+$.

7-(1,1-Dimethylheptyl)-1-ethyl-1,4-dihydro-4,4-dimethylchromeno[4,3-*c*]pyrazol-9-ol (13a) and 7-(1,1-dimethylheptyl)-2-ethyl-2,4-dihydro-4,4-dimethylchromeno[4,3-*c*]pyrazol-9-ol (13b): Prepared from **6** (35 mg, 0.1 mmol) and ethylhydrazine oxalate (15.00 mg, 0.1 mmol) by following the procedure described for **9a** and **9b**. Column chromatography on silica gel (hexanes/EtOAc 2:1) allowed isolation of the two isomers **13a** and **13b**. Compound **13a** was obtained as a pale-yellow oil (5.00 mg, 18%); ^{1}H NMR ($CDCl_3$): δ = 8.77 (bs, 1H, OH), 7.37 (s, 1H, 3-H), 6.58 (d, J = 1.6 Hz, 2H, 6-H), 6.49 (d, J = 1.6 Hz, 1H, 8-H), 4.67 (q, J = 7.1 Hz, 2H, NCH_2CH_3), 1.57 (s, 6H, $OC(CH_3)_2$), 1.58–1.47 (m, 2H, NCH_2CH_3), 1.44 (t, J = 7.1 Hz, 3H, 2′-H), 1.23 (s, 6H, $C(CH_3)_2$), 1.17 (bs, 6H, 3′-H, 4′-H and 5′-H), 1.07 (bs, 2H, 6′-H), 0.84–0.78 ppm (m, 3H, 7′-H); ^{13}C NMR ($CDCl_3$): δ = 154.6 (9-C), 153.1 (5a-C), 151.67 (7-C), 133.1 (3-C), 132.2 (9b-C), 123.4 (3a-C), 108.8 (8-C), 108.0 (6-C), 103.2 (9a-C), 76.7 ($OC(CH_3)_2$), 48.4 (NCH_2CH_3), 44.8 (2′-C), 38.1 ($C(CH_3)_2$), 32.1, 30.4 and 25.01 (3′-C, 4′-C and 5-C), 29.0 ($C(CH_3)_2$), 27.7 ($OC(CH_3)_2$), 23.0 (6′-C), 16.3 (2′-C), 14.4 ppm (7′-C); HPLC–MS: [A, 80→100%], t_R = 3.08 min, (99%); MS (ES$^+$, m/z) 371 (100%) [M+H]$^+$; Anal. calcd for $C_{23}H_{34}N_2O_2$: C 74.55, H 9.25, found: C 74.63, H 9.19. Compound **13b** was obtained as a white solid (23 mg, 61%); mp: 160–164 °C; ^{1}H NMR ($CDCl_3$): δ = 8.32 (s, 1H, OH), 7.13 (s, 1H, 3-H), 6.57 (d, J = 1.5 Hz, 8-H), 6.48 (s, 1H, J = 1.5 Hz, 6-H), 4.16 (q, 2H, J = 7.2 Hz, NCH_2CH_3), 1.60 (s, 6H, $OC(CH_3)_2$), 1.56 (bs, 2H, 2′-H), 1.50 (t, 2H, J = 7.2 Hz, NCH_2CH_3), 1.24 (s, 6H, $C(CH_3)_2$), 1.17 (bs, 6H, 3′-H, 4′-H and 5′-H), 1.01–0.96 (m, 2H, 6′-H), 0.86–79 ppm (m, 3H, 7′-H); ^{13}C NMR ($CDCl_3$): δ = 153.6 (9-C), 153.2 (5a-C), 152.9 (7-C), 142.7 (9b-C), 122.8 (3-C), 120.3 (3a-C), 106.9 (6-C), 106.7 (8-C), 101.7 (9a-C), 76.4 ($OC(CH_3)_2$), 47.4 (NCH_2CH_3), 44.9 82(2′-C), 32.2, 30.4 and 30.1 (3′-C, 4′-C and 5′-C), 29.3 ($C(CH_3)_2$), 25.0 ($OC(CH_3)_2$), 23.1 (6′-C), 15.9 (NCH_2CH_3), 14.5 ppm (7′-C); HPLC–MS: [A, 80→100%], t_R = 5.6 min, (98%); MS (ES$^+$, m/z) 371 (100%) [M+H]$^+$; Anal. calcd for $C_{23}H_{34}N_2O_2$: C 74.55, H 9.25, found: C 74.23, H 9.41.

1-(3,4-Dichlorophenyl)-7-(1,1-dimethylheptyl)-1,4-dihydro-4,4-dimethylchromeno[4,3-*c*]pyrazol-9-ol (14a): Prepared from **6** (17.0 mg, 0.05 mmol) and 3,4-dichlorophenylhydrazine hydrochloride (10.0 mg, 0.05 mmol) by following the procedure described for **7**. Column chromatography on silica gel (hexanes/EtOAc 2:1) afforded **14a** as an orange solid (9 mg, 40%); mp: 124–126 °C; ^{1}H NMR ($CDCl_3$): δ = 7.65 (d, J = 2.3 Hz, 1H, 2-H_{phenyl}), 7.50 (s, 1H, 3-H), 7.43 (d, J = 8.5 Hz, 1H, 5-H_{phenyl}), 7.25 (dd, J = 2.3 Hz, J = 8.5 Hz, 1H, 6-H_{phenyl}), 6.66 (d, J = 1.6 Hz, 1H, 6-H), 6.24 (d, J = 1.6 Hz, 1H, 8-H), 1.68 (s, 6H, $OC(CH_3)_2$), 1.60–1.54 (m, 2H, 2′-H), 1.22 (s, 6H, $C(CH_3)_2$), 1.20–1.09 (m, 6H, 3′-H, 4′-H and 5′-H), 1.08–1.02 (m, 2H, 6′-H), 0.84 ppm (t, J = 6.5 Hz, 3H, 7′-H); ^{13}C NMR ($CDCl_3$): δ = 154.6 (9-C), 154.0 (5a-C), 150.0 (7-C), 142.3 (1-C_{phenyl}), 135.3 (3-C), 133.2 (3-C_{phenyl}), 132.2 (9b-C), 130.4 (4-C_{phenyl}), 126.5 (5-C_{phenyl}), 125.4 (2-C_{phenyl}), 123.9 (6-C_{phenyl}), 109.6 (6-C), 108.0 (8-C), 102.4 (9a-C), 76.2 ($OC(CH_3)_2$), 44.7 (2′-C), 38.3 ($C(CH_3)_2$), 32.1, 30.3 and 25.0 (3′-C, 4′-C and 5′-C), 28.9 ($C(CH_3)_2$), 27.7 ($OC(CH_3)_2$, 23.0 (6′-C), 14.5 ppm (7′-C); HPLC–MS: [A, 80→100%], t_R = 5.6 min, (98%); MS (ES$^+$, m/z) 487 (100%) [M+H]$^+$.

1-(2,4-Dichlorophenyl)-7-(1,1-dimethylheptyl)-1,4-dihydro-4,4-dimethylchromeno[4,3-*c*]pyrazol-9-ol (15a): Prepared from **6** (0.05 mg, 0.16 mmol) and 2,4-dichlorophenylhydrazine hydrochloride (0.13 g, 0.63 mmol) by following the procedure described for **7**. Column chromatography on silica gel (hexanes/EtOAc 2:1) afforded **15a** as an orange oil (0.06 g, 75%); ^{1}H NMR ($CDCl_3$): δ = 7.43 (s, 1H, 3-H), 7.39 (d, J = 2.2 Hz, 1H, 3-H_{phenyl}), 7.27 (dd, J = 2.2 Hz, J = 8.7 Hz, 1H, 5-H_{phenyl}), 7.21 (d, J = 8.7 Hz, 1H, 6-H_{phenyl}), 6.56 (d, J = 1.6 Hz, 1H, 6-H), 6.12 (d, J = 1.6 Hz, 1H, 8-H), 1.64 (s, 6H, $OC(CH_3)_2$), 1.46–1.41 (m, 2H, 2′-H), 1.16–1.08 (m, 12H, 3′-H, 4′-H, 5′-H and $C(CH_3)_2$), 1.12–0.98 (m, 2H, 6′-H), 0.82 ppm (t, J = 6.9 Hz, 3H, 7′-H); ^{13}C NMR ($CDCl_3$): δ = 154.3 (9-C), 153.6 (5a-C), 151.3 (7-C), 140.3 (1-C_{phenyl}), 135.3 (2-C_{phenyl}), 135.0 (4-C_{phenyl}), 134.4 (3-C), 133.0 (9b-C), 129.8 (3-C_{phenyl}), 129.6 (5-C_{phenyl}), 127.3 (6-C_{phenyl}), 123.4 (3a-C), 108.8 (6-C), 107.6 (8-C), 102.6 (9a-C), 77.6 ($OC(CH_3)_2$), 44.7 (2′-C), 39.1 ($C(CH_3)_2$), 32.1, 30.3 and 24.9 (3′-C, 4′-C and 5′-C), 28.9 ($C(CH_3)_2$), 28.0 ($OC(CH_3)_2$), 23.0 (6′-C), 14.5 ppm (7′-C); HPLC–MS: [A, 20→80%], t_R = 19.0 min, (99%); MS (ES$^+$, m/z) 487 (100%) [M+H]$^+$.

Biological studies

Binding evaluation: Membranes from transfected cells expressing human CB_1 or CB_2 cannabinoid receptors (RBHCB1M400UA and RBXCB2M400UA) were supplied by PerkinElmer Life and Analytical Sciences (Boston, MA, USA). The CB_1 receptor membrane protein concentration was 2.33 or 3.60 pmol mg^{-1} depending on the

batch, and the protein concentration was 8.0 mg mL^{-1}. The CB_2 receptor membrane protein concentration was 5.20 or 6.20 pmol mg^{-1}, and the protein concentration was 4.0 or 3.6 mg mL^{-1} depending on the batch. The commercial membranes were diluted (~1:20) with binding buffer (50 mM TrisCl, 5 mM $MgCl_2{\cdot}H_2O$, 2.5 mM EDTA, 0.5 mg mL^{-1} BSA, and pH 7.4 for CB_1 binding; 50 mM TrisCl, 5 mM $MgCl_2{\cdot}H_2O$, 2.5 mM EGTA, 1 mg mL^{-1} BSA, and pH 7.5 for CB_2 binding). The final membrane protein concentration was 0.4 mg mL^{-1} incubation volume and 0.2 mg mL^{-1} incubation volume for CB_1 and CB_2 receptor assays, respectively. The radioligand used was [^{3}H]CP55940 (PerkinElmer) at a concentration of membrane $K_D \times 0.8$ nm, and the final volume was 200 μL for CB_1 binding and 600 μL for CB_2 binding; 96-well plates and tubes necessary for the experiment were previously siliconized with Sigmacote (Sigma).

Membranes were resuspended in the corresponding buffer and were incubated with the radioligand and test compound (10^{-4}–10^{-11} M) for 90 min at 30 °C. Nonspecific binding was determined with 10 μM WIN 55,212-2, and 100% binding of the radioligand to the membrane was determined by its incubation with membrane without test compound. Filtration was performed by a Harvester filtermate (PerkinElmer) with Filtermat A GF/C filters pretreated with 0.05% polyethylenimine. After filtering, the filter was washed with binding buffer (9×0.2 mL for CB_1 and 9×0.6 mL for CB_2), dried, and a melt-on scintillation sheet (Meltilex A, PerkinElmer) was melted onto it. Radioactivity was then quantified by liquid scintillation spectrophotometry (Wallac MicroBeta Trilux, PerkinElmer). Competition binding data were analyzed by using GraphPad Prism software; K_i values are expressed as the mean ± SEM of at least three experiments performed in triplicate for each point.

Isolated tissue assays: Compounds **11**, **13a**, and **13b** were evaluated with mouse vas deferens preparations. This is a nerve-smooth muscle preparation that serves as a highly sensitive and quantitative functional in vitro bioassay for cannabinoid receptor agonists. These ligands induce a concentration-related decrease in the amplitude of electrically evoked contractions of the vas deferens by acting on naturally expressed prejunctional neuronal cannabinoid receptors to inhibit the release of the contractile neurotransmitters noradrenalin and ATP provoked by the electrical stimulation.[47,48] For this study, male ICR mice weighing 25–30 g were used. Mouse vas deferens were isolated as described by Hughes et al.[49] Tissues were suspended in a 10 mL organ bath containing 5 mL Krebs solution (NaCl 118 mM, KCl 4.75 mM, $CaCl_2$ 2.54 mM, KH_2PO_4 1.19 mM, $MgSO_4$ 1.2 mM, $NaHCO_3$ 25 mM, and glucose 11 mM), which was continuously purged with 95% O_2 and 5% CO_2. Tissues were kept under 0.5 g resting tension at 37 °C and were electrically stimulated through two platinum ring electrodes. They were subjected to alternate periods of stimulation (trains of five rectangular pulses of 70 V, 15 Hz, and 2 ms duration each, were applied every minute) and rest (10 min). The isometric force was monitored by a MacLab data recording and analysis system.

The effect of the synthetic cannabinoid agonists arachidonyl-2-chloroethylamide (ACEA), WIN 55,212-2, and that of the new compounds **11**, **13a**, and **13b** (10^{-7}–1.8×10^{-5} M) was tested by constructing concentration–response curves for them in a step-by-step manner. Curves were carried out by the following protocol: ACEA, WIN 55,212-2, or the new compounds were added at a dose to the organ bath 50 min after the beginning of electrical stimulation, and their effect on the electrically induced contractions was evaluated 10 min after addition. Electrical stimulation was then stopped, the Krebs solution was replaced, and the following dose of the compounds was added. This protocol was repeated for every dose. To test the involvement of the CB_1 and CB_2 receptors in the effect of **13a**, this compound was tested in tissues incubated with the respective cannabinoid antagonists AM251 or AM630 (10^{-6} M). Concentration–response curves for the new compound were constructed in a step-by-step manner as follows: AM251 or AM630 was added to the organ bath 50 min after the beginning of electrical stimulation, and 10 min later a dose of **13a** was added; its effect on the electrically induced contractions was monitored 10 min later. Electrical stimulation was then stopped, the Krebs solution was replaced, and the cannabinoid receptor antagonist was added again to determine the effect of the following concentration of the new compound. This protocol was repeated for every dose of **13a**. Results were expressed as a percentage of inhibition, taking the mean amplitude of the last five contractions before the first addition of the agonist as 100%. Each tissue was employed to construct only one concentration–response curve.

In vivo behavioral studies: Behavioral testing of cannabinoids was performed to assess psychoactive drug potential, CNS side effects, as well as medicinal potential. Compound **13a** was evaluated in tests of CNS activity by using the mouse cannabinoid tetrad. The potential antinociceptive effect was also evaluated in an orofacial pain model, induced by hypertonic saline (HS).

Animals: ICR male mice (25–30 g) and Wistar male rats (250–300 g), purchased from Harlan S.A. (Santa Perpetua de Mogoda, Spain), were used in cannabinoid tetrad and orofacial pain model, respectively. Animals were supplied with food and water ad libitum and were housed in a temperature-controlled room at 23 ± 1 °C under a standard 12 h light/dark cycle (08:00–20:00); they were housed in the test room for at least two days before experimentation. Throughout the experimental procedure, the international ethics standards for pain-inducing experiments in laboratory animals[50] and the European Communities Council Directive of 24 November 1986 (86/609 EEC, Nov. 24, 1986) were followed. All animal procedures were reviewed and approved by the Animal Care and Use Committee of Rey Juan Carlos University.

Drugs: WIN 55,212-2 and compound **13a** were dissolved in ethanol (1 mg mL^{-1}) and subsequently in ethanol and Tween 80 (1:2), after which the ethanol was evaporated and saline solution added to reach final concentration.[47] All solutions were made fresh before each experiment.

Cannabinoid tetrad: The classical cannabinoid tetrad was performed to study CNS side effects; this test evaluates antinociception, hypothermia, catalepsy, and locomotor activity in the same animal 20 min after cannabinoid administration.[51] Separated groups of mice ($n \geq 10$) were i.p. treated with vehicle, WIN 55,212-2 (2.5 and 5 mg kg^{-1}) and compound **13a** (5 and 10 mg kg^{-1}). Tests were consecutively conducted with an interval of 5 min between them.

Antinociception: The hot-plate test was carried out using a hot plate at 55 °C as nociceptive stimulus. The latency time for licking of the front paw was taken as an index of nociception. The latency was measured before treatment (control latency) and after every treatment (latency after treatment). The cutoff time was 30 s, and analgesia was quantified with the formula of the maximum possible effect (MPE), expressed as a percentage:

$$\%\,\mathrm{MPE} = \frac{(\text{latency after treatment}) - (\text{control latency})}{(\text{cutoff time}) - (\text{control latency})} \times 100.$$

Hypothermia: Core temperatures in mice were measured using a P6 thermometer and a lubricated rectal probe (Cibertec, Madrid, Spain) inserted into the rectum at a constant depth of 1 cm. Data were recorded before and 30 min after treatment.

Catalepsy: Catalepsy was measured using a modified "ring test", originally described by Pertwee.[51] Mice were placed on a rubber-coated metal ring ($\varnothing = 6$ cm) fixed horizontally at a height of 30 cm. The amount of time in which the mouse is immobile after placement on the ring is recorded for 5 min, and it is considered as an index of catalepsy.

Locomotor activity: Motor coordination was assessed with the rotarod test (Cibertec, Madrid, Spain), in which mice were required to walk against the motion of a rotating drum with a constant speed of 10 rpm over the course of 5 min. The time (s) taken to fall was recorded as latency. Animals were trained to the rotarod test before the pharmacological assay. On the day of the drug test, rotarod latencies were measured immediately before the drug or vehicle was given and 30 min after drug injection. In all experiments a 300 s cutoff time was used; this time was assigned a value of 100% for locomotor activity.

Orofacial pain model: The injection of 100 μL HS (5% NaCl) in the masseter of lightly anesthetized rats produces ipsilateral hindpaw shaking behavior that is accepted as an index of muscle nociception.[45,46,52] Separated groups of rats ($n \geq 10$) were i.p. treated with the vehicle or compound **13a** (1–3 mg kg^{-1}) 30 min after HS was injected in the masseter. Shaking behavior was quantified by counting the total number of shakes over a 2 min period after the intramuscular injection of HS. To count the number of shakes, the experiments were recorded on video and then played back in slow motion.

Molecular modeling

Amino acid numbering: The numbering scheme for class A GPCRs suggested by Ballesteros and Weinstein[53] was employed herein. In this system, the most highly conserved residue in each TMH is assigned a locant of 0.50. This number is preceded by the TMH number and followed in parentheses by the sequence number. All other residues in a TMH are numbered relative to this residue.

Conformational analysis of 11 and 13a/13b: Global minimum energy conformations of **11** and **13a/13b** were determined with Spartan '04 as follows: the structure of each molecule was built from the fragment library available in the program. Ab initio energy minimizations of each structure (HF 6-31G*) were then performed. A conformational search was next performed using Spartan '04 (Monte Carlo method) followed by a minimization of the energy of each conformer at the semiempirical PM3 level. For this search, selected bonds were allowed to rotate: C–O bond in the phenolic ring, the first two C–C bonds of the dimethylheptyl chain, and the N–C bond in the ethyl substituent of the pyrazole, in the case of **13a** and **13b**. Representative conformers according to their geometry were selected for ab initio energy minimization (HF 6-31G*), the global minimum-energy conformer of each was used in docking studies.

Docking with CB_1R*: Binding site anchoring interactions within the receptor for each ligand were based on earlier published docking studies for HU210.[38] Lys3.28(192) was used as the primary interaction site for the phenolic hydroxy group of each chromenopyrazole. Mutation of this residue in CB_1 results in the loss of binding of classical, non-classical, and endocannabinoids, suggesting that interaction with K3.28 is crucial for binding of this class of ligand.[41] The energy of the ligand–CB_1R* TMH bundle complex was minimized using the OPLS2005 force field in Macromodel 9.1 (Schrödinger Inc., Portland, OR, USA). An 8.0 Å extended nonbonded cutoff (updated every 10 steps), a 20.0 Å electrostatic cutoff, and a 4.0 Å hydrogen bond cutoff were used in each stage of the calculation; 7000 steps of conjugate gradient minimization in 500-step increments (six times) followed by 1000-step increments (four times) were employed in a distance-dependent dielectric. A 100 kJ mol^{-1} restraint was placed on all ϕ and ψ angles in TMH1–7 and helix 8, and a 50 kJ mol^{-1} restraint was placed on the Lys3.28(192)–phenolic OH hydrogen bond.

Energy expense assessments for docked ligands: To calculate the energy difference between the global minimum-energy conformer of each compound and its final conformation after energy minimization of the ligand–receptor complex, rotatable bonds in the global minimum-energy conformation were driven to their corresponding value in the final docked conformation, and the single-point energy of the resultant structure was calculated at the HF 6-31G* level using Jaguar (implemented in Maestro 8.5, Schrödinger).

Docking in CB_2R*: Global minimum-energy conformations of each ligand were superimposed on HU210 in its complex with the CB_2R* model (unpublished results). Benzopyran atoms of **14** and **16a/b** were selected for superimposition with benzopyran atoms of HU210. The conformation of the 1,1-dimethylheptyl side chain in the HU210–CB_2R* complex was used to overlay the 1,1-dimethylheptyl side chain position of **11** and **13a/b**. After the superimposition, HU210 was removed. The pyrazole ring of the chromenopyrazoles ligands all had steric clashes with the Asp275/Lys3.28(109) salt bridge. Changes in side chain dihedrals of these two residues were attempted to relieve the steric overlaps; however, it was impossible to relieve this clash without disrupting this ionic lock.

Assessment of pairwise interaction energies: After defining the atoms of each ligand as one group (Group 1) and the atoms corresponding to a residue that lines the binding site in the final ligand–CB_1R* complex as another group (Group 2), Macromodel (version 8.6, Schrödinger, LLC, New York, NY, USA) was used to output the pairwise interaction energy (coulombic and van der Waals) for a given pair of atoms. The pairs corresponding to Group 1 (ligand) and Group 2 (residue of interest) were then summed to yield the interaction energy between the ligand and that residue.

Acknowledgements

We gratefully acknowledge research support from Spanish Grant SAF 2009-12422-C02-02, CANNAB-CM (S-SAL-0261-2006 and S2010-BMD-2308), and RTA (RETICS RD06/001/0014) to P.G. and N.J. L.H.-F. and P.M. are respective recipients of a Postdoctoral Contract (ref. JAEDoc-07-00204) and a JAE-Pre Fellowship (ref. JAEPre-2010-01119) from C.S.I.C.

Keywords: agonists · cannabinoids · peripheral · protein models · receptors

[1] J. Gertsch, R. G. Pertwee, V. Di Marzo, *Br. J. Pharmacol.* **2010**, *160*, 523–529.
[2] Y. Gaoni, R. Mechoulam, *J. Am. Chem. Soc.* **1971**, *93*, 217–224.
[3] R. G. Pertwee, *Br. J. Pharmacol.* **2006**, *147*, S163–S171.
[4] R. G. Pertwee, *Pharmacol. Ther.* **1997**, *74*, 129–180.
[5] K. Mackie, *J. Neuroendocrinol.* **2008**, *20*, 10–14.
[6] L. O. Hanus, R. Mechoulam, *Curr. Med. Chem.* **2010**, *17*, 1341–1359.
[7] K.-S. C. Marriott, J. W. Huffman, *Curr. Top. Med. Chem.* **2008**, *8*, 187–204.

[8] N. Jagerovic, C. Fernandez-Fernandez, P. Goya, *Curr. Top. Med. Chem.* **2008**, *8*, 205 – 230.
[9] K. Woelkart, O. M. Salo-Ahen, R. Bauer, *Curr. Top. Med. Chem.* **2008**, *8*, 173 – 186.
[10] R. G. Pertwee, *Br. J. Pharmacol.* **2009**, *156*, 397 – 411.
[11] S. Pavlopoulos, G. A. Thakur, S. P. Nikas, A. Makriyannis, *Curr. Pharm. Des.* **2006**, *12*, 1751 – 1769.
[12] V. Di Marzo, M. Bifulco, L. De Petrocellis, *Nat. Rev. Drug Discovery* **2004**, *3*, 771 – 784.
[13] G. Appendino, G. Chianese, O. Taglialatela-Scafati, *Curr. Med. Chem.* **2011**, *18*, 1085 – 1099.
[14] G. A. Thakur, S. P. Nikas, A. Makriyannis, *Mini Rev. Med. Chem.* **2005**, *5*, 631 – 640.
[15] G. A. Thakur, S. P. Nikas, C. Li, A. Makriyannis, *Handb. Exp. Pharmacol.* **2005**, 209 – 246.
[16] G. A. Thakur, R. I. Duclos, Jr., A. Makriyannis, *Life Sci.* **2005**, *78*, 454 – 466.
[17] S. L. Palmer, G. A. Thakur, A. Makriyannis, *Chem. Phys. Lipids* **2002**, *121*, 3 – 19.
[18] J. W. Huffman, J. R. Miller, J. Liddle, S. Yu, B. F. Thomas, J. L. Wiley, B. R. Martin, *Bioorg. Med. Chem.* **2003**, *11*, 1397 – 1410.
[19] J. W. Huffman, S. Yu, V. Showalter, M. E. Abood, J. L. Wiley, D. R. Compton, B. R. Martin, R. D. Bramblett, P. H. Reggio, *J. Med. Chem.* **1996**, *39*, 3875 – 3877.
[20] M. H. Rhee, Z. Vogel, J. Barg, M. Bayewitch, R. Levy, L. Hanus, A. Breuer, R. Mechoulam, *J. Med. Chem.* **1997**, *40*, 3228 – 3233.
[21] A. Mahadevan, C. Siegel, B. R. Martin, M. E. Abood, I. Beletskaya, R. K. Razdan, *J. Med. Chem.* **2000**, *43*, 3778 – 3785.
[22] A. D. Khanolkar, D. Lu, M. Ibrahim, R. I. Duclos, Jr., G. A. Thakur, T. P. Malan, Jr., F. Porreca, V. Veerappan, X. Tian, C. George, D. A. Parrish, D. P. Papahatjis, A. Makriyannis, *J. Med. Chem.* **2007**, *50*, 6493 – 6500.
[23] R. D. Sofia, H. B. Vassar, L. C. Knobloch, *Psychopharmacologia* **1975**, *40*, 285 – 95.
[24] P. J. Welburn, G. A. Starmer, G. B. Chesher, D. M. Jackson, *Psychopharmacologia* **1976**, *46*, 83 – 85.
[25] L. Booker, P. S. Naidu, R. K. Razdan, A. Mahadevan, A. H. Lichtman, *Drug Alcohol Depend.* **2009**, *105*, 42 – 47.
[26] J. Sanders, D. M. Jackson, G. A. Starmer, *Psychopharmacology* **1979**, *61*, 281 – 5.
[27] F. Petitet, B. Jeantaud, P. Bertrand, A. Imperato, *Eur. J. Pharmacol.* **1999**, *374*, 417 – 421.
[28] R. W. Steger, L. L. Murphy, A. Bartke, M. S. Smith, *Pharmacol. Biochem. Behav.* **1990**, *37*, 299 – 302.
[29] J. B. Press, G. H. Birnberg, *J. Heterocycl. Chem.* **1985**, *22*, 561 – 564.
[30] S. J. Dominianni, C. W. Ryan, C. W. DeArmitt, *J. Org. Chem.* **1977**, *42*, 344 – 346.
[31] J. Lim, I.-H. Kim, H. H. Kim, K.-S. Ahn, H. Han, *Tetrahedron Lett.* **2001**, *42*, 4001 – 4003.
[32] J. B. Press, J. J. McNally, P. J. Sanfilippo, M. F. Addo, D. Loughney, E. Giardino, L. B. Katz, R. Falotico, B. J. Haertlein, *Bioorg. Med. Chem.* **1993**, *1*, 423 – 435.
[33] B. Loev, P. E. Bender, F. Dowalo, E. Macko, P. J. Fowler, *J. Med. Chem.* **1973**, *16*, 1200 – 1206.
[34] N. Jagerovic, L. Hernandez-Folgado, I. Alkorta, P. Goya, M. Navarro, A. Serrano, F. R. de Fonseca, M. T. Dannert, A. Alsasua, M. Suardiaz, D. Pascual, M. I. Martin, *J. Med. Chem.* **2004**, *47*, 2939 – 2942.
[35] D. R. Compton, K. C. Rice, B. R. Decosta, R. K. Razdan, L. S. Melvin, M. R. Johnson, B. R. Martin, *J. Pharmacol. Exp. Ther.* **1993**, *265*, 218 – 226.
[36] P. H. Reggio, *Handb. Exp. Pharmacol.* **2005**, 247 – 281.
[37] D. P. Hurst, A. Grossfield, D. L. Lynch, S. Feller, T. D. Romo, K. Gawrisch, M. C. Pitman, P. H. Reggio, *J. Biol. Chem.* **2010**, *285*, 17954 – 17964.
[38] A. Kapur, D. P. Hurst, D. Fleischer, R. Whitnell, G. A. Thakur, A. Makriyannis, P. H. Reggio, M. E. Abood, *Mol. Pharmacol.* **2007**, *71*, 1512 – 1524.
[39] N. M. Nebane, D. P. Hurst, C. A. Carrasquer, Z. Qiao, P. H. Reggio, Z. H. Song, *Biochemistry* **2008**, *47*, 13811 – 13821.
[40] Y. Pei, R. W. Mercier, J. K. Anday, G. A. Thakur, A. M. Zvonok, D. Hurst, P. H. Reggio, D. R. Janero, A. Makriyannis, *Chem. Biol.* **2008**, *15*, 1207 – 1219.
[41] Z. H. Song, T. I. Bonner, *Mol. Pharmacol.* **1996**, *49*, 891 – 896.
[42] R. Zhang, D. P. Hurst, J. Barnett-Norris, P. H. Reggio, Z. H. Song, *Mol. Pharmacol.* **2005**, *68*, 69 – 83.
[43] Y. Cheng, S. A. Hitchcock, *Expert Opin. Invest. Drugs* **2007**, *16*, 951 – 65.
[44] Q. Tao, S. D. McAllister, J. Andreassi, K. W. Nowell, G. A. Cabral, D. P. Hurst, K. Bachtel, M. C. Ekman, P. H. Reggio, M. E. Abood, *Mol. Pharmacol.* **1999**, *55*, 605 – 613.
[45] E. B. A. Sánchez, A. Bagües, M. I. Martín, *Pharmacol. Biochem. Behav.* **2010**, *96*, 488 – 495.
[46] S. R. Han, M. K. Lee, K. H. Lim, G. Y. Yang, H. J. Jeon, J. S. Ju, Y. W. Yoon, S. K. Kim, D. K. Ahn, *Eur. J. Pain* **2008**, *12*, 361 – 370.
[47] R. G. Pertwee, L. A. Stevenson, D. B. Elrick, R. Mechoulam, A. D. Corbett, *Br. J. Pharmacol.* **1992**, *105*, 980 – 984.
[48] A. Thomas, R. G. Pertwee, *Methods Mol. Med.* **2006**, *123*, 191 – 207.
[49] J. Hughes, H. W. Kosterlitz, F. M. Leslie, *Br. J. Pharmacol.* **1975**, *53*, 371 – 381.
[50] M. Zimmermann, *Pain* **1983**, *16*, 109 – 110.
[51] R. G. Pertwee, *Br. J. Pharmacol.* **1972**, *46*, 753 – 763.
[52] J. Y. Ro, N. Capra, R. Masri, *Pain* **2003**, *104*, 179 – 185.
[53] J. A. Ballesteros, H. Weinstein, *Methods in Neurosciences* (Eds.: P. M. Conn, S. M. Sealfon), Academic Press, San Diego, **1995**, pp. 366 – 428.

Received: November 30, 2011
Revised: January 18, 2012
Published online on February 2, 2012

